The Structure of LNA:DNA Hybrids from Molecular Dynamics Simulations: The Effect of Locked Nucleotides†

Anela Ivanova‡ and Notker Rösch*

Department Chemie, Theoretische Chemie, Technische Universität München, 85747 Garching, Germany

Received: April 25, 2007; In Final Form: July 13, 2007

Locked nucleic acids (LNAs) exhibit a modified sugar fragment that is restrained to the C3′-endo conformation. LNA-containing duplexes are rather stable and have a more rigid structure than DNA duplexes, with a propensity for A-conformation of the double helix. To gain detailed insight into the local structure of LNA-modified DNA oligomers (as a foundation for subsequent exploration of the electron-transfer capabilities of such modified duplexes), we carried out molecular dynamics simulations on a set of LNA:DNA 9-mer duplexes and analyzed the resulting structures in terms of base step parameters and the conformations of the sugar residues. The perturbation introduced by a single locked nucleotide was found to be fairly localized, extending mostly to the first neighboring base pairs; such duplexes featured a B-type helix. With increasing degree of LNA modification the structure gradually changed; the duplex with one complete LNA strand assumed a typical A-DNA structure. The relative populations of the sugar conformations agreed very well with NMR data, lending credibility to the validity of the computational protocol.

Introduction

Synthetic oligonucleotides recently have been subject to intensive research as they offer possibilities of fine-tuning their properties for a wide range of bio-oriented applications. Modified nucleotide building blocks with intriguing structural and physicochemical characteristics have been synthesized.[1,2] Among them, locked nucleic acids (LNA) are most promising for RNA and DNA mimetics.[3−5]

LNA monomers contain a modified sugar residue with an additional bridge (Figure 1a),[5,6] which confines the furanose ring to N-type conformation, natural for the A-form of DNA and RNA duplexes in helix form. This modification entails a more rigid structure of the phosphate backbone but does not prevent hybrization of LNA strands with complementary RNA or DNA. On the contrary, as monitored by melting temperatures, duplexes are substantially more stable when hybrized with LNA.[4−6] Structural changes in LNA:DNA or LNA:RNA helices with respect to pure DNA:DNA or DNA:RNA duplexes have been observed experimentally.[3,5,7,8] The actual conformation (A-form, B-form or a mixture thereof) depends on the fraction of locked monomers: the greater the amount of LNA nucleotides, the more prominent is the A-DNA form.

The enhanced stability of LNA-containing materials, combined with low toxicity and uncomplicated synthesis and processing, has triggered their industrial-scale production. A multitude of bioapplications of LNA materials has recently been reported.[9] These include usage of LNA assemblies as PCR primers[10] and agents affecting RNase H activity[7,11] as well as applications as LNAzymes,[12] and in antisense and antigene therapeutics.[2,13] Also, LNA has been proposed to be used in diagnostics via microarrays targeting RNA.[14]

Fairly unexplored is the potential utilization of LNA for designing nanostructured materials, directed in particular toward molecular electronics. Currently, various DNA oligonucleotides and their supramolecular assemblies are designed and aimed to function as molecular wires or parts of other "molecular" devices.[15] The charge-transfer properties of DNA, based on electron transfer (ET) between the nucleobases, have been

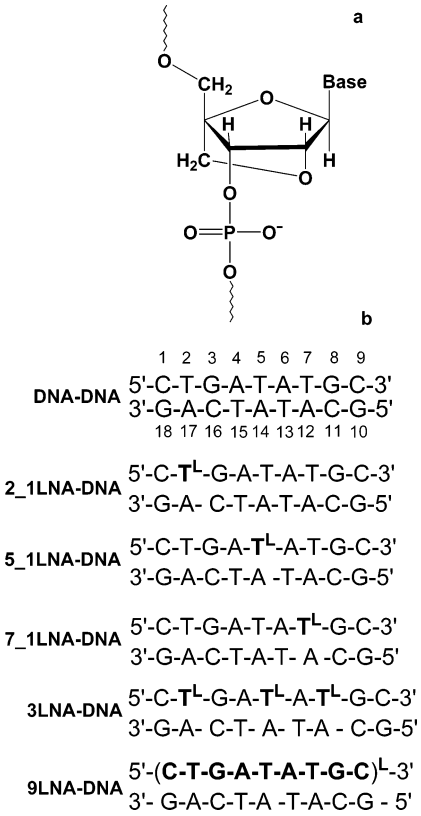

Figure 1. (a) Sketch of a locked sugar residue; (b) base pair sequences of the 9-mer duplexes studied, together with the numbering of the nucleotides. Upper indices L indicate locked monomers.

† Part of the "Sheng Hsien Lin Festschrift".

* Corresponding author. E-mail: roesch@ch.tum.de.

‡ On leave from University of Sofia, Faculty of Chemistry, Department of Physical Chemistry, 1 J. Bourchier Avenue, 1164 Sofia, Bulgaria.

10.1021/jp073198j CCC: $37.00
Published on Web 08/25/2007

intensely studied experimentally and theoretically.[16,17] In view of conformational changes induced by introducing LNA modifications into DNA double helices, ET characteristics of such macromolecules may be altered as well. To quantify the structure-sensitive ET properties,[16a,18] one needs detailed knowledge of the local structures of π-stacks in LNA:DNA duplexes.

A series of LNA:RNA and LNA:DNA duplexes and their unmodified analogues have been explored by NMR.[8,19−23] Combination of COSY, NOESY, and NOE NMR spectra has helped to unravel the structures of LNA duplexes in solution. X-ray crystallographic and AFM studies of such compounds have also been reported.[24] The type of helical structure, the arrangement of the phosphate backbone, as well as sugar conformations of nonlocked nucleotides were resolved for a series of LNA-containing duplexes.[8,19−24]

In all these NMR investigations,[19−23] restrained molecular dynamics (rMD) simulations were used to extract helical parameters, distances between phosphorus atoms, and phosphate backbone dihedral angles as well as to visualize the experimental structures. Sugar conformations of the nonmodified nucleotides were determined from DQF COSY *J*-constants. Thus far, there are hardly purely theoretical studies of LNA-modified duplexes. Very recently, the enhanced stability of LNA-containing hybrids was rationalized via DFT estimates of binding energies in a set of base pair trimers comprising DNA, RNA, LNA, and PNA; yet, one should note that these models did not include effects of an electrolyte environment.[25]

Specific information on the structure of LNA:DNA duplexes at the molecular level is still missing. For instance, one would like to understand from systematic "molecular modeling" studies how an increasing content of LNA nucleotides affects local structural characteristics of the π-stack, sugar puckering variables, etc. In the present paper, we report on unrestrained molecular dynamics (MD) simulations for a series of LNA:DNA duplexes and the corresponding unmodified DNA:DNA reference system. We characterize all systems by base step parameters (BSP)[26] as geometric descriptors to quantify the effect of an increasing fraction of LNA nucleotides on the helical structure. We also discuss how the structure of a duplex is affected by the location of the LNA modification. Furthermore, we address the geometry of the sugar moieties in terms of the conformation of the furanose ring and the puckering amplitude.

Molecular Models and Computational Details

Structural parameters from rMD calculations targeting experimental results[19−23] provide a practical reference for validating a simulation protocol for LNA systems. Therefore, as initial objects of our unrestrained MD simulations, we chose a set of six 9-mer duplexes, all *with the same sequence of nucleotides* (Figure 1b). Three duplexes were selected from the structures investigated experimentally (NMR),[20−22] namely an unmodified DNA:DNA reference duplex, a partially modified LNA:DNA complex containing three locked thymidine nucleotides, and its analogue with one fully modified LNA strand. In addition, we modeled three singly modified 9-mers, each with one locked thymidine nucleotide. For each of these six systems, the base pair sequence and the numbering of the corresponding 18 nucleotides are shown in Figure 1b.

The chosen set of structures allowed us to estimate the influence of increasing LNA modification on the geometry of mixed duplexes. Locking single thymidine nucleotides at different positions along the DNA strand illustrates the importance (if any) of placing locked fragments in the center or near the end of a helix. Moreover, from studying duplexes with a single LNA modification, we expected clues regarding the range of the LNA-induced structural perturbation.

Molecular dynamics simulations were performed with the program package NAMD 2.6.[27] In all calculations, we used the force field AMBER95,[28a] augmented with torsional parameters[28b] that yield an improved presentation of DNA fragments. Although recent findings indicate that the polarizable version of this force field reproduces better agreement with experimental structures,[28c] the nonpolarizable *ff*99 variant was used in this work because it allows direct comparison with rMD simulations performed earlier for some of the studied oligomers.[20−22]

For calculating the electrostatic contribution to the potential energy, one needs suitable atomic charges. We applied the recommended RESP scheme[29] to the locked nucleotides (LNs). We followed the procedure described for standard nucleic acids where atomic charges had been fitted to the electrostatic potential generated at the HF/6-31G* level.[29c] First, at the B3LYP/6-31G* level of theory,[30] we separately optimized the geometries of all four neutral locked nucleosides and of the dimethylphosphate anion in gauche−gauche conformation, for all of which we then calculated the HF/6-31G* electrostatic potential. Subsequently, using the module RESP of Amber 8,[31] we carried out a multimolecule RESP fitting separately for each locked nucleoside and a phosphate moiety. The resulting atomic charges of the four locked monomers and the corresponding phosphates (see Figure S1 of Supporting Information) were used in all simulations. At variance with the original scheme,[29c] we did not average the charges of the four locked sugars and the corresponding phosphate moieties but used them as obtained for each LN because this reflects better the chemical specificity of each monomer. Although the exact charge values differ from those implemented in the force field for conventional nucleic acids, positively and negatively charged centers are preserved and the relative polarity of the different nucleotide fragments is the same. Not unexpectedly, the differences in the electron density distribution are largest in the sugar ring. The center C2′ becomes more positive due to its bond with the newly introduced bridging oxygen, whereas the neighboring methylene group reduces the positive charge on the center C4′. The RESP atomic charges produced in this work are in general very close to those previously employed in rMD simulations.[22]

The initial structure of the reference DNA duplex was constructed in B-DNA form with the program NAB.[32,33] The modified duplexes were obtained by substituting locked nucleotides in the reference duplex. We introduced sodium cations to neutralize the phosphate charges. Duplex and counterions were solvated by TIP3P water molecules[34] and enclosed in a rectangular periodic box that was taken to extend about 10 Å from the solute in each direction. Force field parameters, topology, and Cartesian coordinates of the resulting structures were obtained with the LEaP module of Amber 8.[31] The unit cells thus obtained contain ∼3300 water molecules and consist of ∼11 000 atoms in total. The dimensions of the periodic boxes are between 50 and 60 Å. Table S1 (Supporting Information) summarizes parameters pertinent to the size of the simulated systems.

Before running an MD simulation, each initial structure was subjected to 10 000 steps of conjugate gradient energy minimization. During the subsequent equilibration, we invoked an NVT ensemble.[35] During 20 ps, the system was heated from 0 to 298 K and then maintained at 298 K for 130 ps. For each duplex, equilibration was followed by NPT MD production runs of 10 ns with time steps of 2 fs. The trajectories were generated at 298 K temperature and 1 atm pressure. In all MD simulations,

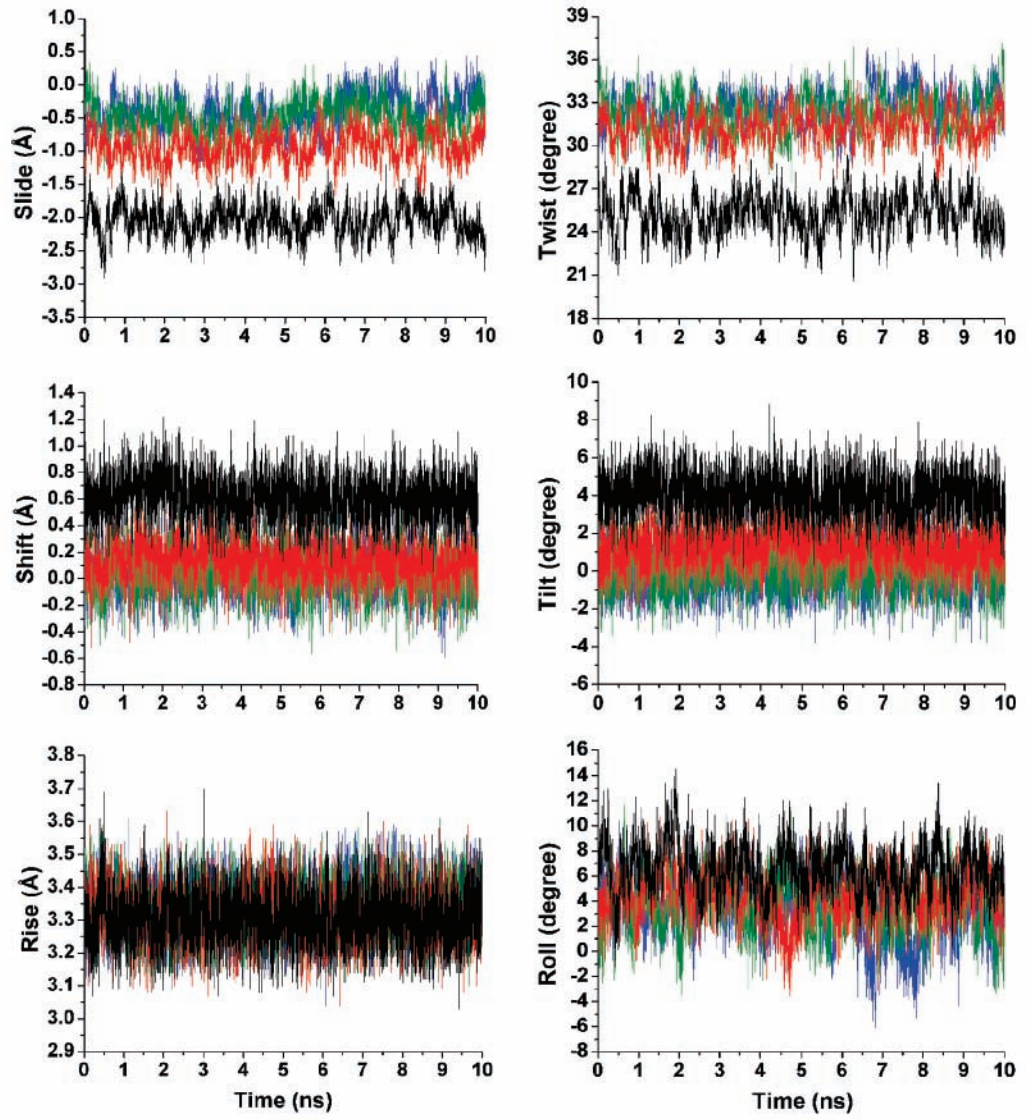

Figure 2. Averages of the six base pair step parameters for selected duplexes, displayed along the corresponding trajectories: 10 000 snapshots extracted at intervals of 1 ps: blue, **DNA−DNA**; green, **5_1LNA−DNA**; red, **3LNA−DNA**; black, **9LNA−DNA**.

a particle mesh Ewald (PME) technique[36] was used to estimate electrostatic interactions; a cutoff of 10 Å (switched on at 8 Å) was applied to the direct part of the PME sum and to nonbonded interactions. All hydrogen-containing bonds in the duplexes were constrained with the SHAKE algorithm[37] and those in water with the procedure SETTLE.[38] We invoked standard AMBER scaling factors for 1−4 electrostatic and nonbonded interactions. We checked the stability of MD simulations by monitoring fluctuations of the total energy and the density as well as of temperature and pressure.

The resulting MD trajectories were subjected to structural analysis to quantify the DNA structure and its change upon introduction of locked nucleotides. With the help of the program 3DNA,[26b] we characterized the geometry of the duplexes by evaluating the six base step parameters (three distances *rise*, *shift*, *slide*, and three angles *tilt*, *twist*, *roll*) and by determining the conformation of the sugar moieties. Note that, unless explicitly specified, we will discuss *local* base step parameters (BSPs). We also calculated B-factors using the utility PTRAJ of the Amber 8 package. All quantities were statistically analyzed for ensembles of 10 000 snapshots that had been extracted from the trajectories at intervals of 1 ps.

To verify that the average BSP values for the various duplexes, albeit close in some cases, stem from different statistical distributions, we carried out two-sided *t* tests, comparing pairs of average values for one and the same BSP. In 52 out of 54 cases, we obtained *p* values lower than 0.05 (see Table S2 of Supporting Information). Thus, the differences of these averages are significant within the standard confidence interval of 95%. The two exceptions concern the rise values of **5_1LNA−DNA** and **7_1LNA−DNA** when compared to those of **DNA−DNA**. Thus, statistical analysis showed that the trends observed in our simulations represent meaningful structural changes.

Results and Discussion

We discuss the structure of the oligomers studied in terms of three types of parameters. We start with a *global* analysis of the structure by monitoring how averages of BSPs over various duplexes change along the trajectories. Then, for each duplex, we analyze trajectory averages of BSPs of individual neighboring base pairs. Finally, we compare BSPs and sugar conformations to experimental data.

TABLE 1: Averages and Standard Deviations of Base Step Parameters for All Duplexes Studied along the Corresponding Trajectories[a]

duplex	shift	slide	rise	tilt	roll	twist
DNA−DNA	0.06 ± 0.16	−0.42 ± 0.27	3.33 ± 0.07	0.2 ± 1.1	3.2 ± 2.3	32.5 ± 1.3
2̄1LNA−DNA	0.07 ± 0.16 (0.01)	−0.63 ± 0.25 (0.21)	3.31 ± 0.07 (0.02)	0.6 ± 1.1 (0.4)	3.8 ± 2.1 (0.6)	31.8 ± 1.2 (0.7)
5̄1LNA−DNA	0.05 ± 0.17 (0.01)	−0.49 ± 0.25 (0.07)	3.33 ± 0.07 (0.00)	0.2 ± 1.1 (0.0)	3.7 ± 2.1 (0.5)	32.3 ± 1.3 (0.2)
7̄1LNA−DNA	0.10 ± 0.16 (0.04)	−0.59 ± 0.27 (0.17)	3.33 ± 0.08 (0.00)	0.7 ± 1.1 (0.5)	3.1 ± 2.2 (0.1)	32.5 ± 1.4 (0.0)
3̄LNA−DNA	0.13 ± 0.16 (0.07)	−0.94 ± 0.25 (0.52)	3.31 ± 0.08 (0.02)	1.4 ± 1.2 (1.2)	4.3 ± 1.9 (1.1)	31.2 ± 1.2 (1.3)
9LNA−DNA	0.61 ± 0.16 (0.55)	−2.05 ± 0.22 (1.63)	3.31 ± 0.08 (0.02)	4.1 ± 1.1 (3.9)	6.5 ± 2.1 (3.3)	25.3 ± 1.3 (7.2)
B-DNA[b]	0.00	−0.19	3.36	0.0	−2.8	36.0
A-DNA[c]	0.00	−1.70	3.28	0.0	10.8	31.0

[a] Experimental values for B-DNA and A-DNA helices are also shown for comparison. Relative absolute changes of average base step parameters with respect to the reference **DNA−DNA** duplex are given in parentheses. distances in Å, angles in deg. [b] Reference 33. [c] Reference 39.

Base Step Parameters along Trajectories. For a subset of the LNA:DNA 9-mer duplexes, Figure 2 presents the time evolution of average base step parameters (taken over all base steps of a duplex) as derived from the snapshots along the MD trajectories. For each duplex studied, Table 1 summarizes *overall* averages of each BSP (for all base pair steps of each duplex over all snapshots) of the three translational and the three rotational base step parameters. The corresponding average parameters of canonical B-DNA[33] and A-DNA,[39] also calculated with the program 3DNA, are provided for comparison. Inspection of Figure 2 and Table 1 reveals that the six BSP values of all systems fall into ranges that are typical for DNA helices.

In terms of BSP values, the structure of the nonmodified **DNA−DNA** reference duplex is close to that of standard B-DNA.[33] The largest differences between calculated and experimental average values occur for slide (0.23 Å) and roll (6°) (Table 1). The experimental data correspond to averaged parameters of an "ideal" B-DNA duplex. The differences in slide and roll, however, come from the specific nucleotide sequence in the oligomers studied. The larger negative slide is due to the two (AT)(TA) steps, and the big positive roll stems from the (TA)(GC) and (TA)(AT) steps. That specific behavior of these steps agrees with experimental results.[40] Nevertheless, more than 80% of the structures of the reference exhibit the characteristics of B-DNA as judged by the program 3DNA via the qualifiers Zp and ZpH.[26b] None of the six parameters seems to exhibit a special trend along the trajectory, only more or less random fluctuations around their averages (Supporting Information, Tables S3 and S4). However, base pairs 5 and 6 in the middle of the duplex appear to be relatively mobile, as the standard deviations of their BSPs are among the largest (see also the discussion of B-factors below). On the basis of the above, the simulated DNA:DNA duplex is considered suitable as reference for comparison with the analogous LNA:DNA 9-mers.

The base pair step parameters averaged over LNA-containing duplexes (Figure 2) exhibit a similar behavior along the trajectories as the corresponding parameters of the DNA reference. All parameters fluctuate randomly around their average values without any specific patterns along the trajectories that would indicate systematic structural changes.

However, for slide, shift, twist, and tilt, one observes systematic differences between 9-mer duplexes with increasing number of locked monomers (Figure 2). Slide is most sensitive to locking among the three distance BSPs, to be followed by shift; similarly, twist is most sensitive among the angle parameters, to be followed by tilt. This can be seen from the different relative displacements of the corresponding curves and will be discussed in more detail in the next section. Values of roll also change, but to a much smaller extent, while alterations in rise with LN content are not noticeable on the scale of the graphs (Figure 2, Table 1, Tables S3 and S4 of Supporting Information). The *pattern* of change of the parameters along the duplex is most robust for roll because its values are closer to those in A-DNA already in the reference duplex and do not need major readjustments upon LNA modification. The absolute values of slide, shift, roll, and tilt clearly increase with the fraction of LNs, and values of twist and rise decrease concomitantly (Table 1). The largest standard deviations among the distance BSPs were calculated for slide and among the angles for roll. This is in line with statistics on experimental X-ray structures[40] where these two BSPs, together with twist, were classified as least restricted among the six BSPs.

Comparison between the base step parameters of the three *singly modified* 9-mers is provided as Supporting Information (Figure S2). As shown by the standard geometric descriptors, all duplexes evolve quite regular along the trajectories. As discussed above, only slide, roll, and twist fluctuate in a more noticeable fashion around their average values. However, the range of values spanned by a given BSP is the same for the three helices, e.g., slide varies between −1.4 and 0.2 Å and twist changes from 28° to 36° in all singly modified systems. Averages of BSP values over duplexes and trajectories (Table 1) are very similar to those of the reference **DNA−DNA**, thus indicating that a single LN perturbation is not strong enough to change appreciably the overall helical structure. Neither does the location of the LN modification on the strand induce differences in the average characteristics of the entire hybrids.

The mean difference between the overall average characteristics of **DNA−DNA** and **3LNA−DNA** is 0.20 Å for translational BSPs and 1.2° for angular BSPs. These values are slightly larger than the sum of the changes due to the three single LNs (rows 2−5 of Table 1). The corresponding mean differences between **9LNA−DNA** and **DNA−DNA** is 0.73 Å and 4.8°, which are larger than three times the changes observed in **3LNA−DNA**. Thus, structural changes do not seem to be strictly proportional to the number of LNs. Rather, there is some amplification due to the interaction between different LN modifications. This interaction is mostly expressed in terms of shift and twist.

Trends of the BSPs indicate a gradual transformation of the helix structure from B-DNA to A-DNA form due to the effect of locked nucleotides that notably increases with the LN content of the oligomers (Table 1). The fully modified duplex **9LNA−DNA** already has average base step parameters that are characteristic of an A-DNA helix. The overall structural differences between **DNA−DNA** and **9LNA−DNA** are illustrated by Figure 3. The four systems with partial LN modification exhibit intermediate BSP values between those of **DNA−DNA** and **9LNA−DNA** (Table 1). The average values of slide, roll, and tilt of the hybrid with three modified thymine

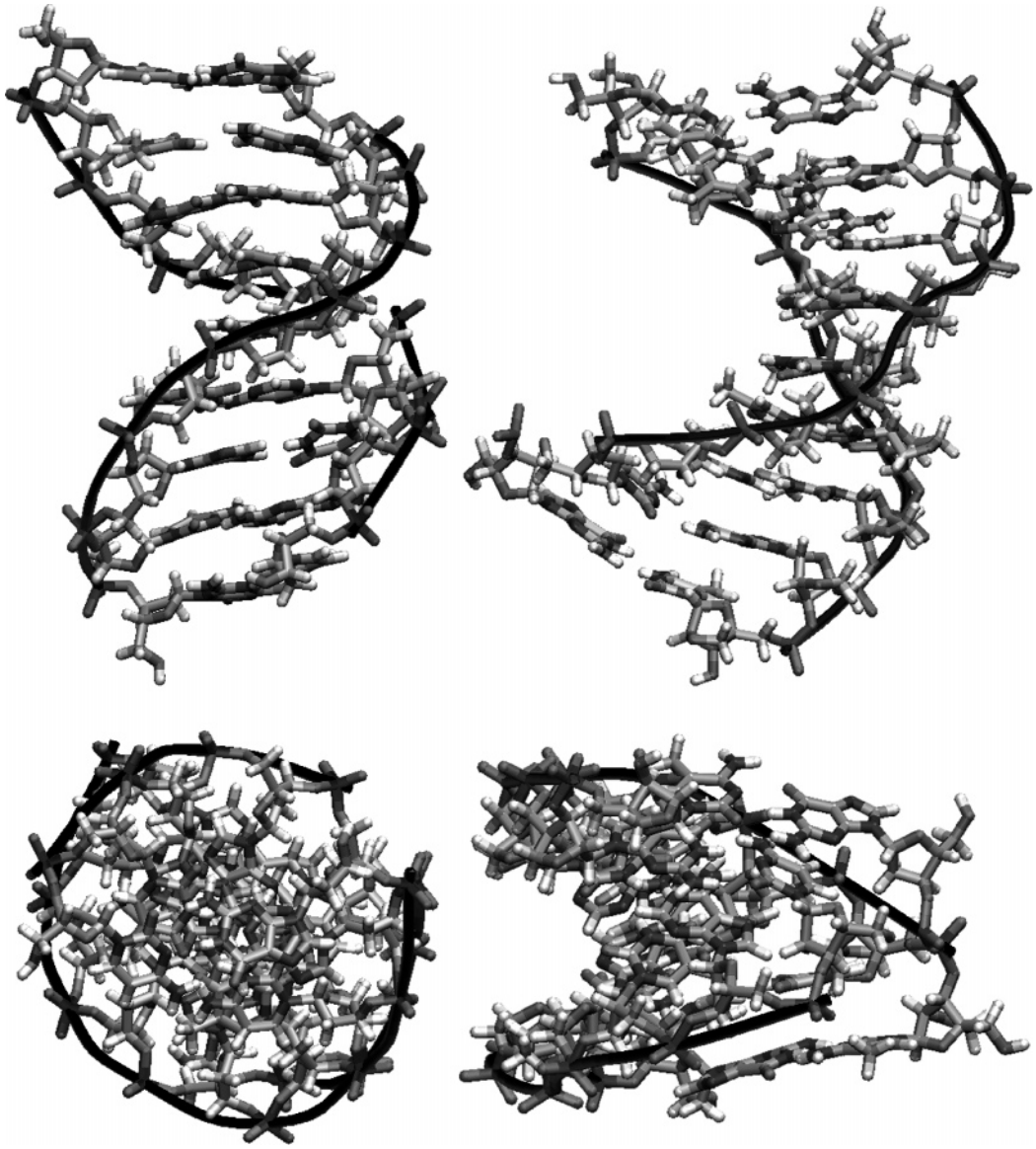

Figure 3. Helix types in **DNA−DNA** (left panel) and **9LNA−DNA** (right panel): typical snapshots with value of the base step parameters close to their averages for the corresponding system.

nucleotides differ from those of the reference, but the remaining BSPs are like those in **DNA−DNA**, i.e., in total, the structure resembles more a B-DNA type (Table 1). Singly modified duplexes have duplex-averaged BSPs (along trajectories, Figure S2 of Supporting Information) and trajectory-averages (Table 1) that are very similar to the corresponding quantities of the **DNA−DNA** reference.

Step Parameters between Individual Base Pairs. Having established how LN content affects the overall shape of the duplexes, we now turn to the trajectory averages of individual base step parameters. Figure 4 shows these data for the six base step parameters in four of the six 9-mers studied.

The trajectory averages of the base step parameters between individual base pairs in **3LNA−DNA** display moderate changes compared to the reference system **DNA−DNA**, while variations are much more pronounced in the fully modified duplex **9LNA−DNA** (Figure 4, Table S3 of Supporting Information).

As has to be expected from the findings for duplex averages, strong systematic BSP deviations for individual base pair steps from **DNA−DNA** to **9LNA−DNA** are observed for slide, shift, twist, tilt, and partially for roll (Figure 4, Tables S3, S4 of Supporting Information). The structure variations in the LNA:DNA duplexes, expressed as differences of BSP values for each base pair step from the corresponding data of **DNA−DNA**, decrease with increasing LN content for the BSPs listed. For example, the largest difference among the distances between **9LNA−DNA** and **DNA−DNA** is for slide of base pair steps 8−9 (2.10 Å) and the smallest one is for rise of base pair steps 6−7 (the two values coincide). Among the angles the corresponding maximum and minimum deviations are for twist of base pair steps 3−4 (17.6°) and for roll of steps 7−8 (0.8°). These finding are in line with the response of those characteristics already observed from the behavior of BSP duplex averages along the various trajectories (Figure 2, Table 1).

On the basis of experimental data on DNA duplexes, by statistical analysis of X-ray structures and by principal component analysis, slide and roll have been classified as BSPs which are most sensitive to structure perturbations.[33,39−41] In our simulations, this is confirmed for the effect of LN content on slide. Roll probably changes less in LNA:DNA oligomers because its values are non-negligible already in the reference DNA−DNA duplex (see below). The most stable characteristic

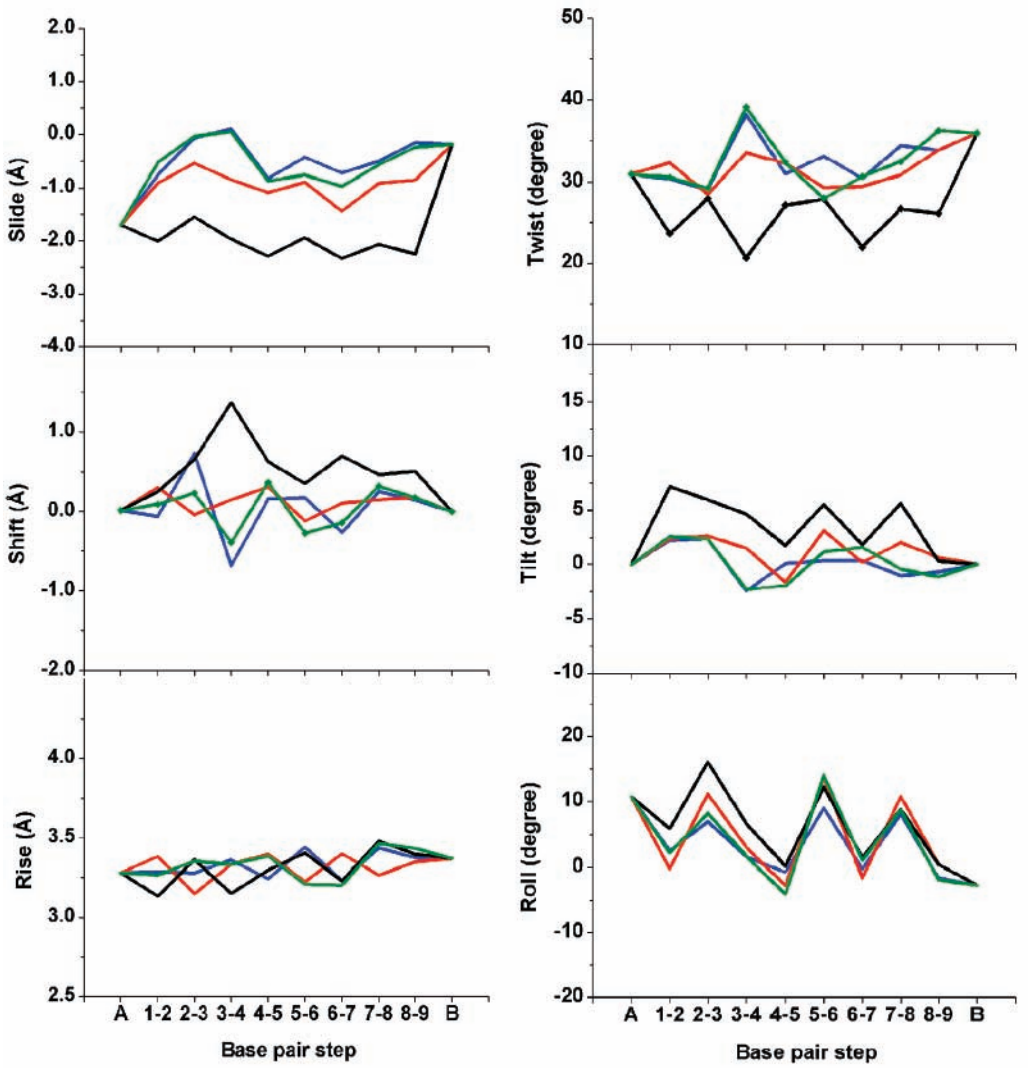

Figure 4. Trajectory averages of individual base pair step parameters in **DNA−DNA** (blue), **5_1LNA−DNA** (green), **3LNA−DNA** (red), and **9LNA−DNA** (black), estimated from MD trajectories of 10 ns. The canonical values of A-DNA and B-DNA are indicated as A and B, respectively.

according to our computations is rise; its fluctuations are smallest and do not seem to be affected by LN content (Figure 4).

The trajectory averages of the individual BSP values (Figure 4) are not uniform along the various duplexes but most likely are governed by chemical specificity of the neighboring base pairs. For example, the two (TA)(GC) steps 2−3 and 7−8 have large roll values in all duplexes; this has also been observed in other MD simulations,[42] theoretical conformational analysis,[43] and in X-ray structures[40] and is partly due to the bulky methyl group of thymine interacting with the sugar methylene group[43] or to specific hydrogen bonds.[40] The notable roll values of the fifth base pair step may have a similar cause[43] but in addition may be associated with the central position in the helix.

Already in **3LNA−DNA** one finds practically all (individual) base step parameters affected by the LN modification because each base pair (except for the CG pair 9−10, Figure 1) has a locked nucleotide as nearest neighbor. For most base pair steps of the triply modified oligomer, the values of slide and roll are merely displaced to larger absolute values relative to the **DNA−DNA** reference and those of twist to smaller values, while the other three parameters change in a less uniform manner. As shown previously,[40] twist and roll are always inversely correlated and the present results are no exception. In **9LNA−DNA**, slide and roll preserve the direction of change compared to **3LNA−DNA**: the former becomes more negative and the latter more positive with respect to the corresponding values of the triply modified duplex. Tilt of all base pair steps in **9LNA−DNA** is also displaced toward more positive values. Thus, the trend of these three parameters is already defined by partial locking of the three thymine nucleotides of **3LNA−DNA**. On the other hand, shift and twist in **9LNA−DNA** exhibit changes of opposite quality with respect to nonmodified or partially modified duplexes: if a value in the latter system is small, then it is large in **9LNA−DNA** and vice versa. This indicates that a more substantial LN modification is necessary for these two parameters to adopt the values characteristic of fully locked duplexes, i.e., positive shift and small twist.

All parameter changes in **9LNA−DNA** are in line with the transition to the helical form of A-DNA[39] as is confirmed by detailed inspection of Table 1 and Table S3 (see Supporting Information). As already mentioned, **9LNA−DNA** has average base step parameters that correspond to the A-DNA type of the helix, while **3LNA−DNA** (with only three locked thymidine nucleotides) still resembles more closely B-DNA than A-DNA helical conformation although its BSP values are intermediate (Table 1). The present limited data sets do not allow a conclusion whether this is a consequence of the non-neighboring placement or simply the amount of LN modifications. In other

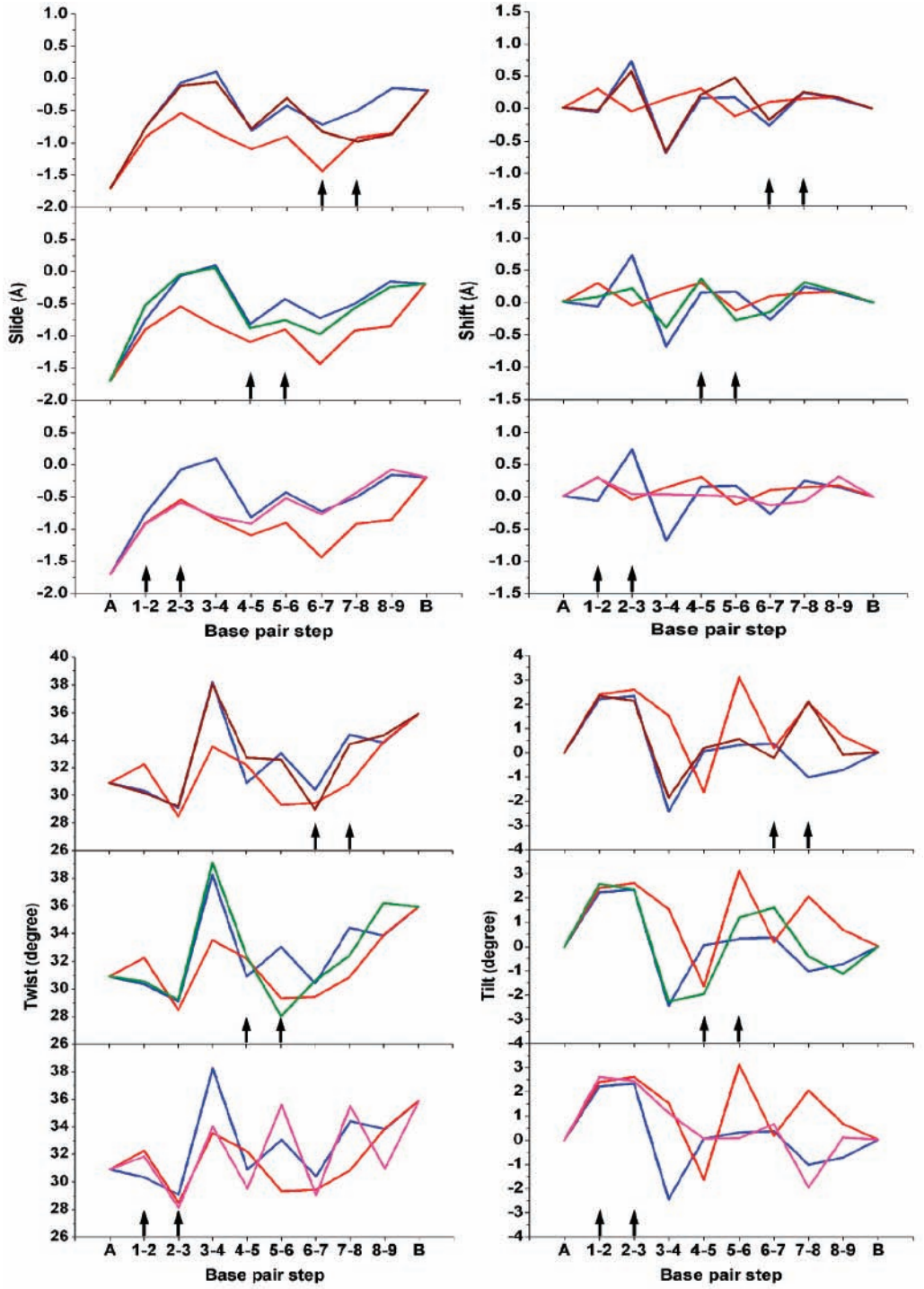

Figure 5. Trajectory averages of the base step parameters shift, slide, tilt, and twist for individual steps of **2_1LNA−DNA** (magenta), **5_1LNA−DNA** (green), and **7_1LNA−DNA** (brown). Results for **DNA−DNA** (blue) and **3LNA−DNA** (red) are given for comparison. The canonical values of A-DNA and B-DNA are indicated as A and B, respectively. The arrows designate the two base pair steps containing locked nucleotides.

words, a substantial change of the overall structure may require a larger fraction of LNA components than just $^1/_3$ as in **3LNA−DNA**.

The BSP values of the three *singly modified* duplexes (Figure 5) very well illustrate how far LN-induced structural perturbations propagate along a duplex. Away from the marked LN-modified regions, all BSPs follow closely the **DNA−DNA** curve (blue). In contrast, the LN-containing steps and their neighbors have BSP values essentially identical to those in **3LNA−DNA**. In fact, for each singly modified duplex, those BSPs involving a LN modification are closer to the **3LNA−DNA** curve (red). Apparently, in the vicinity of the perturbation, the structure of all singly modified duplexes resembles that of **3LNA−DNA**, whereas in the remaining part of the duplex, the BSPs are like those of **DNA−DNA**. This holds for all parameters but is especially evident for slide as the parameter most sensitive to LN modification. Besides base pairs in nearest-neighbor positions to the modification, the step involving the next-nearest base pair in 3′-direction from the LN is also affected. These observations confirm the local nature of the conformation perturbation due to a single LN substitution. Furthermore, adjacent LNs are necessary for nonadditive structural influence that leads to a global change of the helical conformation. Note that the BSPs of the perturbed region of **5_1LNA−DNA** do not

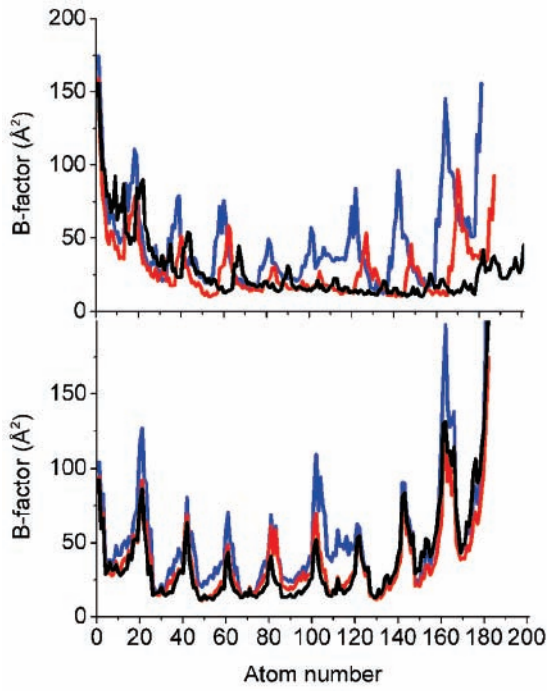

Figure 6. Trajectory-averaged B-factors of heavy atoms of **DNA**−**DNA** (blue), **3LNA**−**DNA** (red), and **9LNA**−**DNA** (black). The upper panel shows the values for strand I (atom numbers increase from residue 1 to residue 9, Figure 1), and the lower panel those for strand II (atom numbers increase from residue 18 to residue 10, Figure 1).

agree with those of **3LNA**−**DNA** to the same degree as those in the two terminally substituted systems. This may be due to reduced flexibility in the center of *this* duplex, which prevents full structural relaxation in response to the LNA modification, at least on the time scale of the present MD simulations. Overall, the three singly modified duplexes have BSPs closer to the average B-DNA values (Table 1, Table S4 of Supporting Information), i.e., the duplexes are in B-DNA form.

From melting point measurements,[4−6] LNA-modified duplexes have been considered as more rigid than their DNA analogues. One wonders how this finding will be reflected in the standard deviations of average structure parameters. The standard deviations of the *individual* base step parameters (Table 1; Tables S3 and S4 and Figure S3 of Supporting Information) in general do not show any trends in the duplexes studied. However, the *duplex-averaged* standard deviations in the LNA:DNA complexes decrease with increasing LNA content, e.g., the standard deviation of slide decreases from 0.59 Å in **DNA**−**DNA** to 0.50 Å in **9LNA**−**DNA** and that of twist from 5.8° to 4.2°. This computational result may be taken to reflect the more rigid nature of LNA modified systems.

The relative rigidity of LNA-containing duplexes is verified by an analysis of the calculated B-factors of all heavy atoms of the three experimentally investigated 9-mer duplexes **DNA**−**DNA**, **3LNA**−**DNA**, and **9LNA**−**DNA** (Figure 6). As expected, the B-factors of all three duplexes are higher for the backbone atoms and lower for those in the bases. However, the increased mobility of base pair step 5−6 (discussed above) of **DNA**−**DNA** is evident: the B-factors for the bases of nucleotides 5, 6, 14, and 15 are substantial. The two terminal base pairs have the highest B-factors, in line with the "fraying" observed experimentally for the three duplexes.[20−22] The absolute values of the obtained B-factors are larger than those normally determined for crystal structures[35] but are comparable to the values recently reported from an MD simulation of a DNA oligomer in solution where the same force field had been used.[28c]

In the two LNA:DNA 9-mers, the B-factors of strand I, which contains the locked nucleotides, are significantly smaller than those of **DNA**−**DNA**. The average B-factors of the atoms in strand I are (45.8 ± 29.4) Å^2 for **DNA**−**DNA**, (29.3 ± 21.0) Å^2 for **3LNA**−**DNA**, and (27.9 ± 22.0) Å^2 for **9LNA**−**DNA**. The mobility of the atoms in the unmodified strand of the two LNA:DNA oligomers is also lower but not as small as in the locked strand. The corresponding average B-factors of strand II are (50.6 ± 37.6) Å^2 for **DNA**−**DNA**, (36.9 ± 25.1) Å^2 for **3LNA**−**DNA**, and (38.2 ± 31.3) Å^2 for **9LNA**−**DNA**.

The adequacy of the computational approach used here can best be judged by comparing structural descriptors from simulations to those extracted from experiment. Therefore, we calculated some *helical* parameters[26b] of **DNA**−**DNA** and **3LNA**−**DNA** and compared them to the corresponding experimental results (Figure S4).[21] *Helical* BSPs differ from the *local* ones discussed above in the coordinate system, which for the latter is based on two mean base pair reference frames in each step, whereas helical BSPs are defined with respect to a helical axis that results from a fit to all equivalent C1′−N9 (purines) and C1′−N1 (pyrimidines) vectors along the same strand.[26b] Thus, helical parameters can be considered as global structural descriptors.

The calculated values of helical rise (h-rise) and twist (h-twist) are similar to those obtained from restrained MD, which can be taken to represent experimental NMR structures of the duplexes (Figure S4).[21] Standard deviations of our trajectory averages are about two times larger than those of "experimental" results. This finding may reflect the unconstrained nature of the present MD simulations, but also the substantially larger ensembles (20 structures in rMD, 10^4 snapshots in the present MD simulations).

In both sets of results, computational and "experimental", h-rise values of the individual steps are more uniform in **DNA**−**DNA** than in **3LNA**−**DNA**. Trends along the duplexes are reproduced as well, except for steps 5−6 in **DNA**−**DNA** and 8−9 in **3LNA**−**DNA**. When discussing differences between theoretical and "experimental" results, one should keep the widely different sizes of the underlying ensembles in mind (see above). The three steps of **3LNA**−**DNA** with a locked nucleotide on the 5′ side (steps 2−3, 5−6, and 7−8) feature smaller h-rise values than the unlocked steps; according to both rMD and unrestricted MD simulations, the differences being more pronounced in the latter structures. MD and rMD data also show similar alterations of h-twist on going from **DNA**−**DNA** to **3LNA**−**DNA** when one compares corresponding base pair steps of the two duplexes; the reduction of h-twist in the LN-modified duplex is most significant for steps 2−3, 5−6, and 7−8. The range of theoretical h-twist values is more compact along the two duplexes. However, there are also notable differences in h-twist between the two data sets: for base steps 6−7 and 7−8 of **DNA**−**DNA** and for 5−6 and 6−7 of **3LNA**−**DNA**, the "experimental" value for 5−6 being very small.[21] These discrepancies may be related to different algorithms for defining the helical axes.[21,26b]

In summary, the helical parameters obtained from the present MD simulations, both for the DNA reference duplex and **3LNA**−**DNA**, in general are more uniform. For **DNA**−**DNA** they are closer to the B-DNA form, and for **3LNA**−**DNA** they are intermediate between B-DNA and A-DNA. Jensen et al. arrived at the same qualitative conclusions on the basis of rMD simulations.[21]

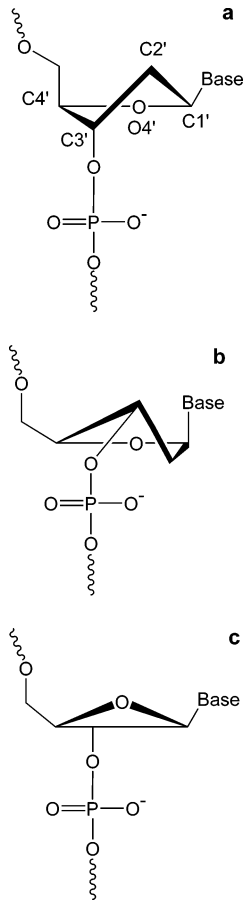

Figure 7. Sugar conformations in DNA and RNA: (a) C2′-endo (S-type), dominant in B-DNA (atom notations in the furanose ring provided); (b) C3′-endo (N-type), dominant in A-DNA and RNA; (c) O4′-endo, intermediate conformation, viewed perpendicular to the plane formed by the four carbon atoms of the ring.

Sugar Conformations. In locked nucleotides, the sugar conformation is fixed to the C3′-endo form (Figure 7). The conformations of the other sugar residues are important descriptors of oligomers with locked fragments. In fact, the fractions of different furanose ring conformations provide an alternative measure for the helix type. Experimentally, the conformation of the sugar ring can be determined by fitting NMR coupling constants derived from DQF-COSY spectra.[19−22] Models with one, two, or several states have been used in this fitting procedure.[22] The most simple model derives the helix conformation only on the basis of the fraction of sugars in O4′-endo conformation (Figure 7). The more such sugars are present, the more the structure resembles an A-type helix. A second approach uses the fractions of C2′-endo and C3′-endo conformations for characterizing the helix type as B-form and A-form, respectively. A third type of model admits all ten conformations (5 exo, 5 endo) of the sugar rings. Wengel and co-workers used the two-state model in their experimental study of sugar conformations in unmodified and two LNA-modified 9-mers and calculated the relative populations of the two most abundant sugar conformations;[20−22] they estimated the C2′-endo population from fits of NMR coupling constants and assigned the remaining part of the sugars to the C3′-endo conformation. We used the program 3DNA[26b] to classify the conformation of the furanose rings; following the convention of Altona and Sundaralingam,[44] this procedure relies on a combination of the five cyclic torsion angles C4′−O4′−C1′−C2′, O4′−C1′−C2′−C3′, C1′−C2′−C3′−C4′, C2′−C3′−C4′−O4′, and C3′−C4′−O4′−C1′ (see Figure 7 for the designation of the atoms).

C2′-endo and C3′-endo sugar conformations are known to interconvert relatively easily in DNA (more than 10 times within 2 ns MD of a B-DNA 20-mer)[42] but less often in RNA (only two events within 2 ns MD of A-RNA of the same oligomer).[35,42,45] There have been both experimental and computational attempts to determine the energy difference between the two minima as well as the energy barrier of the pseudorotation that connects the two structures.[46] The C2′-endo form was found to be lower in energy in DNA, and the C3′-endo conformer is the most stable one in RNA. By using a variety of computational methods, ranging from force-field-based simulations to DFT calculations, one finds the two energy minima separated by 0.3−3.0 kcal/mol in deoxyribonucleosides and 0.6−1.7 kcal/mol in ribonucleosides.[46,47] The corresponding free energy differences, as extracted from NMR experiments, are 0.1−0.5 kcal/mol for deoxyribonucleosides and 0.2−0.8 kcal/mol for ribonucleosides, depending on the nucleobase.[46a,48]

The conversion of the C2′-endo to the C3′-endo conformer takes place via the O4′-endo conformation. The corresponding energy barrier of deoxyribonucleosides has been estimated at 1.6−4.3 kcal/mol by using the same type of computational methods as just discussed.[46b,47] At the same level of theory, the C3′-endo to C2′-endo barrier of ribonucleosides was determined at 1.8−5.0 kcal/mol.[47] A potential of mean force simulation using a model potential predicted a free energy barrier of (2.2 ± 0.2) kcal/mol for deoxyadenosine.[49] Values of the potential energy barrier for nucleosides from NMR data vary between 3.3 kcal/mol (deoxycytosyl)[45a] and 4.7 kcal/mol (ribonucleosides).[50]

It is of interest to check the distribution of sugar conformations in LNA-containing duplexes. Figure 8 provides the calculated fractions of the three types of sugar conformations, separately for each nucleotide, of the DNA:DNA and LNA:DNA duplexes studied (see also Table S5 of Supporting Information). Evidently, the unmodified helix of **DNA−DNA** features a B-type structure as the percentage of S-type furanose rings is very high, (87.3 ± 5.6)% on average.[45] The corresponding amounts in the three singly modified systems are very similar: (83.9 ± 6.4)% of the nonlocked sugars of **2_1LNA−DNA** have S-type conformations, (88.4 ± 4.5)% in **5_1LNA−DNA** and (87.7 ± 6.0)% in **7_1LNA−DNA**.

Despite its larger LN fraction, the number of S-type conformations of the sugar rings remains essentially the same for the nonmodified nucleotides of **3LNA−DNA**, (84.0 ± 7.4)% on average. However, the situation is different in **9LNA−DNA**, where the amount of S-type sugar rings of the nonmodified nucleotides decreases to (57.4 ± 18.5)%. On the other hand, the fraction of N-type furanose of the *nonlocked* nucleotides grows regularly with the LNs of the 9-mer duplexes: (3.3 ± 2.5)% in **DNA−DNA**, (4.8 ± 3.5)% in **2_1LNA−DNA**, (3.5 ± 3.8)% in **5_1LNA−DNA**, (3.5 ± 3.4)% in **7_1LNA−DNA**, (5.5 ± 4.1)% in **3LNA−DNA**, and (11.4 ± 7.4)% in **9LNA−DNA**. Thus, locking some monomers affects also other residues throughout the duplex. Moreover, this influence exhibits a directional preference. In singly modified duplexes, the sugar ring of nucleotides at the 3′-side of a locked nucleotide has a higher propensity for changing its conformation to N-type, while unmodified residues on the 5′-side are hardly affected. In our simulations, the N-type population of the neighboring nucleotide at the 3′-side can reach 20%. This supports the "conformational steering" inherent to locked nucleotides that had been concluded from experimental observations.[3]

The various nucleotides are not uniformly affected. Pyrimidine-bound sugars apparently are more easily converted to

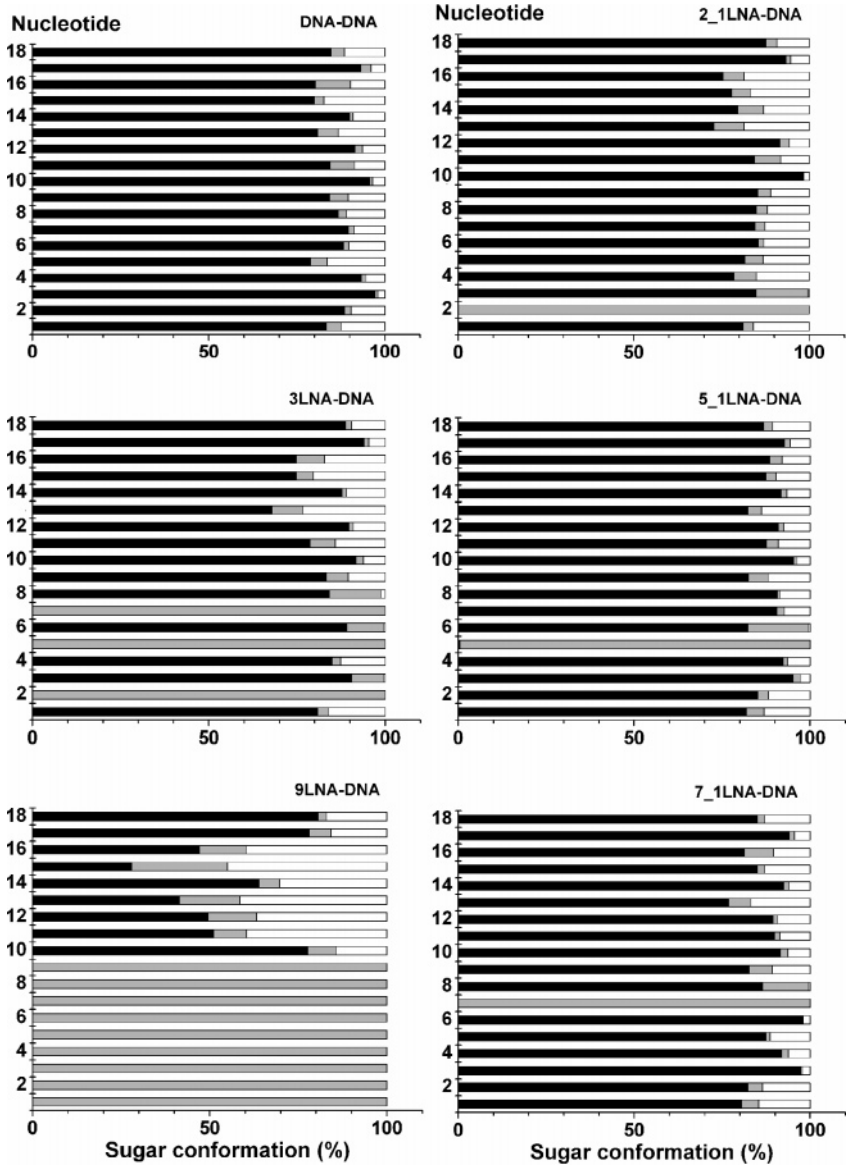

Figure 8. Calculated fractions of sugar conformers in the 9-mer duplexes studied: S-type (black bars), N-type (gray bars), and O4′-endo type (white bars). For the notation of the conformations, see Figure 7.

N-type conformation, while purine-bound sugars are more resistant to conformational change. The distribution of conformations of sugar rings on the nonmodified strand is not systematically altered in partially modified duplexes (Figure 8). However, in the fully modified duplex **9LNA**−**DNA**, more sugar rings of the complementary (DNA) strand are converted to N-type, with populations of up to 30%. As above for base step parameters, also the distribution of sugar conformations is more affected for central moieties of a duplex than for terminal ones. Apparently, the enhanced mobility of terminal residues allows them to adjust more easily their conformation, whereas constraints of central nucleotides limit the possibility for counteracting the structural stress imposed by the more rigid LNA strand.

In the nonlocked strand of **9LNA**−**DNA**, the population of the O4′-endo (intermediate) conformation is notably larger, (31.2 ± 12.2)% on average. Thus, a two-state model may not be optimal for extracting the amount of sugar conformations from NMR data of hybrids with large LN fractions. In **3LNA**−**DNA**, the O4′-endo fraction is comparable to that in **DNA**−**DNA** and singly modified duplexes: (9.4 ± 4.1)% in **DNA**−**DNA**, (11.3 ± 5.5)% in **2_1LNA**−**DNA**, (8.1 ± 3.7)% in **5_1LNA**−**DNA**, (8.8 ± 4.8)% in **7_1LNA**−**DNA**, and (10.5 ± 7.1)% in **3LNA**−**DNA**.

Finally, we turn to a comparison of S-type sugar content from our MD simulations and analogous NMR data[20−22] that are available for most base pairs of the duplexes **DNA**−**DNA**, **3LNA**−**DNA**, and **9LNA**−**DNA** (Figure 9).

Agreement between results from MD simulations and NMR can be considered good for almost all sugar residues if one takes into account error margins of 10−15% of the experimental fractions derived from fits of NMR coupling constants.[20−22] One should not expect full quantitative correspondence between the two sets of values due to the different time scale of the MD simulations, which is shorter than that during which NMR data were accumulated. Striking exceptions to the overall good agreement are residues 4A and 6A of **3LNA**−**DNA** as well as 15T of **9LNA**−**DNA** (Figure 9). These discrepancies may have various reasons. For example, during the fitting of NMR NOE coupling constants, the amplitude of sugar puckering, i.e., the maximum angle of torsion with respect to the plane of the remaining ones,[44] was fixed at 38° in **DNA**−**DNA** and **3LNA**−

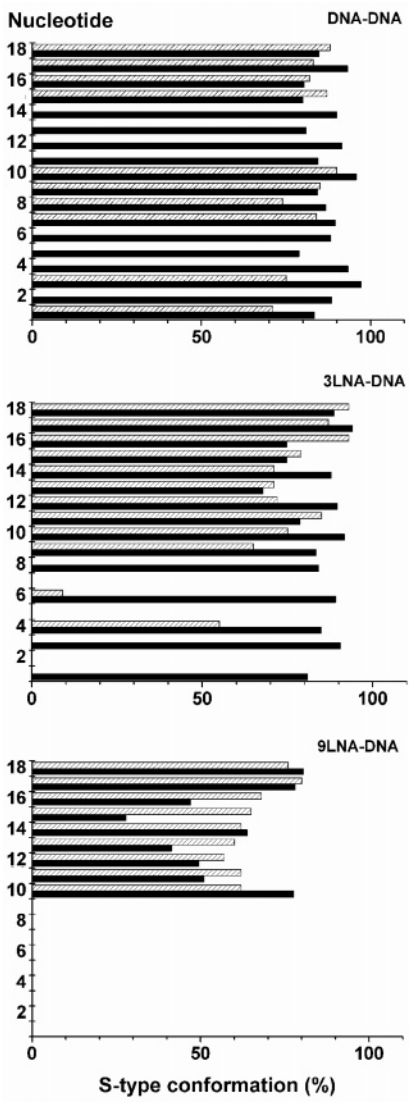

Figure 9. Comparison of S-type sugar contents of individual nucleotides of **DNA**−**DNA**, **3LNA**−**DNA**, and **9LNA**−**DNA** with the available experimental NMR data;[20−22] black bars represent calculated values and white patterned bars experimental ones. For the numbering of the nucleotides see Figure 1.

DNA and at 36° in **9LNA**−**DNA**.[20−22] To check this assumption, we estimated the puckering amplitudes for our MD results and obtained the following average values for the *nonmodified sugars*: (39.3 ± 6.9)° for **DNA**−**DNA**, (37.7 ± 7.0)° for **3LNA**−**DNA**, and (38.8 ± 6.7)° for **9LNA**−**DNA**. Thus, the puckering amplitude is essentially constant and does not depend on the presence or amount of locked nucleotides. All values are similar to the average puckering amplitude in DNA, 39°.[43] In addition, the average puckering amplitudes of the locked sugars are (57.9 ± 3.0)° for **3LNA**−**DNA** and (57.5 ± 3.1)° for **9LNA**−**DNA**, respectively. Thus, sugars of LNs feature larger and more uniform amplitudes, which are necessary for accommodating the second ring fragment. The rigidity of locked sugar is also reflected in the smaller standard deviations; they are less than half of those of standard sugar residues. Although the amplitudes of nonlocked sugars of **9LNA**−**DNA** used in the fitting of experimental data are somewhat different from those calculated here, this does not seem sufficient for rationalizing the observed substantial mismatch in sugar populations of the three nucleotides just mentioned. There also may be problems with evaluating experimental spectra, which exhibit overlapping peaks in the pertinent region, or the short time of the present MD simulations, as mentioned. In this context, note that the analysis of our structure ensembles with respect to average fractions of sugar conformations is statistically stable already with 2500 snapshots.

When averaged over *all* nucleotides of a duplex, experimental estimates of S-type populations, (81.9 ± 6.4)% for **DNA**−**DNA**, (71.3 ± 22.6)% for **3LNA**−**DNA**, (32.9 ± 34.2)% for **9LNA**−**DNA**,[20−22] are not significantly different from our corresponding "theoretical" values: (87.3 ± 5.6)% for **DNA**−**DNA**, (70.0 ± 32.9)% for **3LNA**−**DNA**, and (28.7 ± 32.2)% for **9LNA**−**DNA**. These results support the validity of the computational approach used in this study to provide atomistic characteristics of LNA-modified DNA duplex oligomers.

Conclusions and Outlook

We reported (unconstrained) molecular dynamics simulations on a series of LNA-modified DNA 9-mer duplexes that had been selected because structural information was available via NMR experiments.[20−22] We characterized the structures by a statistical analysis of the six base step parameters of all neighboring base pairs. When tracing the effect of an increasing amount of locked nucleotides, we diagnosed a "gradual" change from B-DNA to A-DNA helix conformation. The system with one fully locked chain displayed as a whole a structure that corresponds to A-DNA form. The current MD results indicate that any structural perturbation due to an isolated (single) locked nucleotide is fairly localized within a duplex, essentially restricted to the immediate neighboring base pairs.

We also determined populations of the three most abundant conformations of the sugar rings. We found the amount of N-type sugars of nonmodified nucleotides to increase with the fraction of locked nucleotides, consistent with the transition to A-DNA helix. Unmodified sugars of nucleotides at the 3′-side of locked nucleotides showed a larger propensity for changing their sugar conformation from S- to N-type, in line with experimental findings.[20−22]

Comparison of structure data for the same LNA-modified 9-mer duplexes, derived either from NMR data or the present unconstrained MD simulations, supports the validity of our computational protocol. Similar MD simulations can generate valuable structural information on LNA-modified DNA duplexes and thus will open the route to further in-depth studies on larger and more complicated LNA:DNA systems of practical interest. Quite a few questions regarding the structure of LNA-modified duplexes remain to be answered. A notable advantage compared to NMR experiments is the relative swiftness with which molecular simulations can provide an atomistic structural description of good quality of prospective LNA-containing oligomers. Ultimately, MD simulations may open the route to effective targeted molecular design for LNA-modified DNA. Moreover, such simulations may even provide geometrical characteristics that are not directly accessible to experimental techniques, e.g., amplitudes of sugar ring puckering of locked nucleotides.

It is intriguing to speculate how the changed base step parameters of LNA-containing duplexes compared to standard DNA duplexes may affect charge transport properties of such duplexes.[16a] After all, the electronic coupling between neighboring base pairs, hence the rate of electron transfer, is known to depend in a very sensitive fashion[16a,17d,18] on the registry of neighboring π-systems.

Acknowledgment. We thank Prof. M.-E. Michel-Beyerle, Dr. Grzegorz Jezierski, and Egor Vladimirov for valuable

suggestions and helpful discussions. A.I. is grateful to the Alexander von Humboldt Foundation for a research fellowship. This work was supported by EC FP6 project NMP4-CT-2003-505669 (STReP CIDNA) and Fonds der Chemische Industrie.

Supporting Information Available: Size of the simulated systems (Table S1), *p*-values from two-sided *t* tests comparing averages of BSPs of different oligomers (Table S2), trajectory-averaged base step parameters of individual base steps in the simulated duplexes (Tables S3, S4), calculated fractions of the three sugar conformations in the oligomers studied (Table S5); RESP atomic charges of locked nucleotides (Figure S1), duplex-averaged base step parameters along the trajectories of singly modified 9-mers (Figure S2), plots of standard deviations of individual base step parameters for a subset of the simulated systems (Figure S3), trajectory-averages of helical rise and twist of individual base pair steps in **DNA−DNA** and **3LNA−DNA** (Figure S4). This material is available free of charge via the Internet at http://pubs.acs.org.

References and Notes

(1) Egli, M.; Gryaznov, S. M. *Cell. Mol. Life Sci.* **2000**, *57*, 1440−1456.

(2) Obika, S. *Chem. Pharm. Bull.* **2004**, *52*, 1399−1404.

(3) Petersen, M.; Wengel, J. *Trends Biotechnol.* **2003**, *21*, 74−81.

(4) Koch, T. *J. Phys.: Condens. Matter* **2003**, *15*, S1861−S1871.

(5) Wengel, J.; Petersen, M.; Frieden, M.; Koch, T. *Lett. Pept. Sci.* **2004**, *10*, 237−253.

(6) (a) Koshkin, A. A.; Singh, S. K.; Nielsen, P.; Rajwanshi, V. K.; Kumar, R.; Meldgaard, M.; Olsen, C. E.; Wengel, J. *Tetrahedron* **1998**, *54*, 3607−3630; (b) Wengel, J. *Acc. Chem. Res.* **1999**, *32*, 301−310.

(7) Bondensgaard, K.; Petersen, M.; Singh, S. K.; Rajwanshi, V. K.; Kumar, R.; Wengel, J.; Jacobsen, J. P. *Chem.−Eur. J.* **2000**, *6*, 2687−2695.

(8) Petersen, M.; Bondensgaard, K.; Wengel, J.; Jacobsen, J. P. *J. Am. Chem. Soc.* **2002**, *124*, 5974−5982.

(9) (a) Orum, H.; Wolter, A.; Kongsbak, L. *Lett. Pept. Sci.* **2004**, *10*, 325−334. (b) Crinelli, R.; Bianchi, M.; Gantilini, L.; Palma, L.; Magnani, L. *Curr. Drug. Targets* **2004**, *5*, 745−752. (c) Jepsen, J. S.; Sorensen, M. D.; Wengel *Oligonucleotides* **2004**, *14*, 130−146.

(10) (a) Latorra, D.; Arar, K.; Hurley, J. M. *Mol. Cell. Probes* **2003**, *17*, 253−259. (b) Maertens, O.; Legius, E.; Speleman, F.; Messiaen, L.; Vandesompele, *J. Anal. Biochem.* **2006**, *359*, 144−146. (c) Levin, J. D.; Fiala, D.; Samala, M. F.; Kahn, J. D.; Peterson, R. J. *Nucleic Acids Res.* **2006**, *34*, e142. (d) Malgoyre, A.; Banzet, S.; Mouret, C.; Bigard, A. X.; Peinnequin, A. *Biochem. Biophys. Res. Commun.* **2007**, *354*, 246−252.

(11) (a) Orom, U. A.; Kauppinen, S.; Lund, A. H. *Gene* **2006**, *372*, 137−141. (b) Lima, W. F.; Rose, J. B.; Nichols, J. G.; Wu, H. J.; Migawa, M. T.; Wyrzykiewicz, T. K.; Vasquez, G.; Swayze, E. E.; Crooke, S. T. *Mol. Pharmacol.* **2007**, *71*, 73−82.

(12) Vester, B.; Hansen, L. H.; Lundberg, L. B.; Babu, B. R.; Sorensen, M. D.; Wengel, J.; Douthwaite, S. *BMC Mol. Biol.* **2006**, *7*, 19.

(13) (a) Kvaerno, L.; Wengel, J. *Chem. Commun.* **2001**, *16*, 1419−1424. (b) Gruegelsiepe, H.; Brandt, O.; Hartmann, R. K. *J. Biol. Chem.* **2006**, *281*, 30613−30620. (c) Swayze, E. E.; Siwkowski, A. M.; Wancewicz, E. V.; Migawa, M. T.; Wyrzykiewicz, T. K.; Hung, G.; Monia, B. P.; Bennett, C. F. *Nucleic Acids Res.* **2007**, *35*, 687−700.

(14) (a) Simeonov, A.; Nikiforov, T. T. *Nucleic Acids Res.* **2002**, *30*, e91. (b) Schmidt, K. S.; Borkowski, S.; Kurreck, J.; Stephens, A. W.; Bald, R.; Hecht, M.; Friebe, M.; Dinkelborg, L.; Erdmann, V. A. *Nucleic Acids Res.* **2004**, *32*, 5757−5765. (c) Yang, C. Y. J.; Medley, C. D.; Tan, W. H. *Curr. Pharm. Biotechnol.* **2005**, *6*, 445−452. (d) Neely, L. A.; Patel, S.; Garver, J.; Gallo, M.; Hackett, M.; McLaughlin, S.; Nadel, M.; Harris, J.; Gullans, S.; Rooke, J. *Nat. Methods* **2006**, *3*, 41−46. (e) Guerasimova, A.; Nyarsik, L.; Liu, J. P.; Schwartz, R.; Lange, M.; Lehrach, H.; Janitz, M. *Biomol. Eng.* **2006**, *23*, 35−40. (f) Darfeuille, F.; Reigadas, S.; Hansen, J. B.; Orum, H.; Di Primo, C.; Toulme, J. J. *Biochemistry* **2006**, *45*, 12076−12082.

(15) (a) Adams, D. M.; Brus, L.; Chidsey, C. E. D.; Creager, S.; Creutz, C.; Kagan, C. R.; Kamat, P. V.; Lieberman, M.; Lindsay, S.; Marcus, R. A.; Metzger, R. M.; Michel-Beyerle, M. E.; Miller, J. R.; Newton, M. D.; Rolison, D. R.; Sankey, O.; Schanze, K. S.; Yardley, J.; Zhu, X. *J. Phys. Chem. B* **2003**, *107*, 6668−6697. (b) Morrison, H. *Bioorganic Photochemistry, Vol. 1: Photochemistry and the Nucleic Acids*; Wiley-Interscience: New York, 1990.

(16) (a) Treadway, C. R.; Hill, M. G.; Barton, J. K. *Chem. Phys.* **2002**, *281*, 409−428. (b) Lewis, F. D.; Wasielewski, M. R. *Top. Curr. Chem.* **2004**, *236*, 45−65. (b) Porath, D.; Cuniberti, G.; Di Felice, R. *Top. Curr. Chem.* **2004**, *237*, 183−227. (c) Lewis, F. D. *Photochem. Photobiol.* **2005**, *81*, 65−72.

(17) (a) Jortner, J.; Bixon, M.; Langenbacher, T.; Michel-Beyerle, M. *Proc. Natl. Acad. Sci. U.S.A.* **1998**, *95*, 12759−12765. (b) Schuster, G. B.; Landman, U. *Top. Curr. Chem.* **2004**, *236*, 139−161. (c) Berlin, Y. A.; Kurnikov, I. V.; Beratan, D; Ratner, M. A; Burin, A. L. *Top. Curr. Chem.* **2004**, *237*, 1−36. (d) Rösch, N.; Voityuk, A. *Top. Curr. Chem.* **2004**, *237*, 37−72.

(18) Voityuk, A. A.; Siriwong, K.; Rösch, N. *Phys. Chem. Chem. Phys.* **2001**, *3*, 5421−5425.

(19) Nielsen, K. E.; Singh, S. K.; Wengel, J.; Jacobsen, J. P. *Bioconjugate Chem.* **2000**, *11*, 228.

(20) Petersen, M.; Nielsen, C. B.; Nielsen, K. E.; Jensen, G. A.; Bondensgaard, K.; Singh, S. K.; Rajwanshi, V. K.; Koshkin, A. A.; Dahl, B. M.; Wengel, J.; Jacobsen, J. P. *J. Mol. Recognit.* **2000**, *13*, 44−53.

(21) Jensen, G. A.; Singh, S. K.; Kumar, R.; Wengel, J.; Jacobsen, J. P. *J. Chem. Soc., Perkin Trans. 2* **2001**, 1224−1232.

(22) Nielsen, K. E.; Rasmussen, J.; Kumar, R.; Wengel, J.; Jacobsen, J. P.; Petersen, M. *Bioconjugate Chem.* **2004**, *15*, 449−457.

(23) Tommerholt, H. V.; Christensen, N. K.; Nielsen, P.; Wengel, J.; Stein, P. C.; Jacobsen, J. P.; Petersen, M. *Org. Biomol. Chem.* **2003**, *1*, 655−663.

(24) (a) Egli, M.; Minasov, G.; Teplova, M.; Kumar, R.; Wengel, J. *Chem. Commun.* **2001**, *7*, 651−652. (b) Forster, C.; Brauer, A. B. E.; Brode, S.; Schmidt, K. S.; Perbandt, M.; Meyer, A.; Rypniewski, W.; Betzel, C.; Kurreck, J.; Furste, J. P.; Erdmann, V. A. *Acta Crystallogr., Sect. F* **2006**, *62*, 665−668. (c) Rinker, S.; Liu, Y.; Yan, H. *Chem. Commun.* **2006**, *25*, 2675−2677.

(25) Natsume, T.; Ishikawa, Y.; Dedachi, K.; Tsukamoto, T.; Kurita, N. *Chem. Phys. Lett.* **2007**, *434*, 133−138.

(26) (a) Diekmann, S. *J. Mol. Biol.* **1989**, *205*, 787−791. (b) X.-J. Lu, W. K. Olson, *Nucleic Acids Res.* **2003**, *31*, 5108−5121.

(27) Phillips, J. C.; Braun, R.; Wang, W.; Gumbart, J.; Tajkhorshid, E.; Villa, E.; Chipot, Ch.; Skeel, R. D.; Kale, L.; Schulten. K. *J. Comput. Chem.* **2005**, *26*, 1781−1802.

(28) (a) Cornell, W. D.; Cieplak, P.; Bayly, C. I.; Gould, I. R.; Merz, K. M., Jr.; Ferguson, D. M.; Spellmeyer, D. C.; Fox, T.; Caldwell, J. W.; Kollman, P. A. *J. Am. Chem. Soc.* **1995**, *117*, 5179−5197. (b) Wang, J.; Cieplak, P.; Kollman, P. A. *J. Comput. Chem.* **2000**, *21*, 1049−1074. (c) Babin, V.; Baucom, J.; Darden, T. A.; Sagui, C. *J. Phys. Chem. B* **2006**, *110*, 11571−11581.

(29) (a) Bayly, C. I.; Cieplak, P.; Cornell, W. D.; Kollman, P. A. *J. Phys. Chem.* **1993**, *97*, 10269−10280. (b) Cornell, W. D.; Cieplak, P.; Bayly, C. I.; Kollman, P. A. *J. Am. Chem. Soc.* **1993**, *115*, 9620−9631. (c) Cieplak, P.; Cornell, W. D.; Bayly, C.; Kollman, P. A. *J. Comput. Chem.* **1995**, *16*, 1357−1377.

(30) Frisch, M. J.; Trucks, G. W.; Schlegel, H. B.; Scuseria, G. E.; Robb, M. A.; Cheeseman, J. R.; Montgomery, J. A., Jr.; Vreven, T.; Kudin, K. N.; Burant, J. C.; Millam, J. M.; Iyengar, S. S.; Tomasi, J.; Barone, V.; Mennucci, B.; Cossi, M.; Scalmani, G.; Rega, N.; Petersson, G. A.; Nakatsuji, H.; Hada, M.; Ehara, M.; Toyota, K.; Fukuda, R.; Hasegawa, J.; Ishida, M.; Nakajima, T.; Honda, Y.; Kitao, O.; Nakai, H.; Klene, M.; Li, X.; Knox, J. E.; Hratchian, H. P.; Cross, J. B.; Bakken, V.; Adamo, C.; Jaramillo, J.; Gomperts, R.; Stratmann, R. E.; Yazyev, O.; Austin, A. J.; Cammi, R.; Pomelli, C.; Ochterski, J. W.; Ayala, P. Y.; Morokuma, K.; Voth, G. A.; Salvador, P.; Dannenberg, J. J.; Zakrzewski, V. G.; Dapprich, S.; Daniels, A. D.; Strain, M. C.; Farkas, O.; Malick, D. K.; Rabuck, A. D.; Raghavachari, K.; Foresman, J. B.; Ortiz, J. V.; Cui, Q.; Baboul, A. G.; Clifford, S.; Cioslowski, J.; Stefanov, B. B.; Liu, G.; Liashenko, A.; Piskorz, P.; Komaromi, I.; Martin, R. L.; Fox, D. J.; Keith, T.; Al-Laham, M. A.; Peng, C. Y.; Nanayakkara, A.; Challacombe, M.; Gill, P. M. W.; Johnson, B.; Chen, W.; Wong, M. W.; Gonzalez, C.; Pople, J. A. *Gaussian 03*, revision C.01; Gaussian, Inc.: Wallingford, CT, 2004.

(31) Case, D. A.; Darden, T. A.; Cheatham, T. E., III; Simmerling, C. L.; Wang, J.; Duke, R. E.; Luo, R.; Merz, K. M.; Wang, B.; Pearlman, D. A.; Crowley, M.; Brozell, S.; Tsui, V.; Gohlke, H.; Mongan, J.; Hornak, V.; Cui, G.; Beroza, P.; Schafmeister, C.; Caldwell, J. W.; Ross, W. S.; Kollman, P. A. *AMBER 8*; University of California: San Francisco, 2004.

(32) Macke, T.; Case, D. A. In *Molecular Modeling of Nucleic Acids*; Leontes, N. B., SantaLucia, J., Jr., Eds.; American Chemical Society: Washington, DC, 1998; p 379.

(33) (a) Arnott, S.; Campbell Smith, P. J.; Chandraseharan, R. In *Handbook of Biochemistry and Molecular Biology*, 3rd ed.; Nucleic Acids: Volume II; Fasman, G. P., Ed.; CRC Press: Cleveland, 1976; pp 411−422. (b) Quintana, J. R.; Grzeskowiak, K.; Yanagi, K.; Dickerson, R. E. *J. Mol. Biol.* **1992**, *225*, 379−395.

(34) Jorgensen, W. L.; Chandrasekhar, J.; Madura, J.; Klein, M. L. *J. Chem. Phys.* **1983**, *79*, 926−935.

(35) Bevan, D. R.; Li, L.; Pedersen, L. G.; Darden, T. A. *Biophys. J.* **2000**, *78*, 668−682.

(36) (a) Darden, T.; York, D.; Pedersen, L. *J. Chem. Phys.* **1993**, *98*, 10089−10092. (b) Essmann, U.; Perera, L.; Berkowitz, M. L.; Darden, T.;

Lee, H.; Pedersen, L. G.; *J. Chem. Phys.* **1995**, *103*, 8577−8593. (c) Toukmaji, A.; Sagui, C.; Board, J.; Darden, T. *J. Chem. Phys.* **2000**, *113*, 10913−10927.

(37) Ryckaert, J.-P.; Ciccotti, G.; Berendsen, H. J. C. *J. Comput. Phys.* **1977**, *23*, 327−341.

(38) Miyamoto, S.; Kollman, P. A. *J. Comput. Chem.* **1992**, *13*, 952−962.

(39) (a) Fuller, W.; Wilkins, M. H. F.; Wilson, H. R.; Hamilton, L. D.; Arnott, S. *J. Mol. Biol.* **1965**, *12*, 60−80. (b) Verdaguer, N.; Aymami, J.; Fernandez-Forner, D.; Fita, I.; Coll, M.; Huynh-Dinh, T.; Igolen, J.; Subirana, J. A. *J. Mol. Biol.* **1991**, *221*, 623−635.

(40) Gorin, A. A.; Zhurkin, V. B.; Olson, W. K. *J. Mol. Biol.* **1995**, *247*, 34−48.

(41) Bharanidharan, D.; Gautham, N. *Biochem. Biophys. Res. Commun.* **2006**, *340*, 1229−1237.

(42) Cheatham, T. E., III; Kollman, P. A. *J. Am. Chem. Soc.* **1997**, *119*, 4805−4825.

(43) Hunter, C. A *J. Mol. Biol.* **1993**, *230*, 1025−1054.

(44) Altona, C.; Sundaralingam, M. *J. Am. Chem. Soc.* **1972**, *94*, 8205−8212.

(45) (a) Meints, G. A.; Karlsson, T.; Drobny, G. P. *J. Am. Chem. Soc.* **2001**, *123*, 10030−10038. (b) Wu, Z.; Delaglio, F.; Tjandra, N.; Zhurkin, V. B.; Bax, A. *J. Biomol. NMR* **2003**, *26*, 297−315. (c) Foloppe, N.; Nilsson, L. *J. Phys. Chem. B* **2005**, *109*, 9119−9131. (d) Gonzales, C.; Stec, W.; Reynolds, M. A.; James, T. L. *Biochemistry* **1995**, *34*, 4969−4982.

(46) (a) Plavec, J.; Tong, W.; Chattopadhyaya, J. *J. Am. Chem. Soc.* **1993**, *115*, 9734−9746. (b) Foloppe, N.; Nilsson, L.; MacKerell, A. D., Jr. *Biopolymers* **2002**, *61*, 61−76.

(47) (a) Olson, W. K. *J. Am. Chem. Soc.* **1982**, *104*, 278−286. (b) Brameld, K. A.; Goddard, W. A., III. *J. Am. Chem. Soc.* **1999**, *121*, 985−993.

(48) Altona, C.; Sundaralingam, M *J. Am. Chem. Soc.* **1973**, *95*, 2333−2344.

(49) Arora, K.; Schlick, T. *Chem. Phys. Lett.* **2003**, *378*, 1−8.

(50) Roder, O.; Ludemann, H.-D.; von Goldammer, E. *Eur. J. Biochem.* **1975**, *53*, 517−525.